Supporting Information

Morphology Graded Silicon Nanowire Arrays via Chemical Etching: Engineering Optical Properties at the Nano- and the Macroscale

Fedja J. Wendisch, [1] *Mehri Abazari,* [1,2] *Hossein Mahdavi,* [2] *Marcel Rey,* [3] *Nicolas Vogel,* [3] *Maurizio Musso,* [1] *Oliver Diwald,* [1] *Gilles R. Bourret* [1,*]

[1] Department of Chemistry and Physics of Materials, University of Salzburg, Jakob Haringer Strasse 2A, A-5020 Salzburg, Austria

[2] School of Chemistry, College of Science, University of Tehran, P.O. Box 14155-6455, Tehran, Iran

[3] Institute of Particle Technology, Friedrich-Alexander University Erlangen-Nürnberg, Cauerstrasse 4, 91058 Erlangen, Germany

*E-mail: gilles.bourret@sbg.ac.at

Table of Content

Table S1: Monosegmented VA-SiNW array dimensions.

The dimensions of all synthesized monosegmented VA-SiNW arrays, shown in the main text, are reported here. All dimensions are in nm.

Monosegmented SiNW Arrays					
Figure	**Array Pitch**	**SiNW Length**	**SiNW Diameter**	**Color**	**Morphology**
2a	418 ± 42	1699 ± 41	118 ± 5	blue	cylinder
2b	428 ± 31	2192 ± 49	87 ± 7	purple	cylinder
2c	437 ± 30	1703 ± 74	77 ± 8	yellow	cylinder
2d	433 ± 27	1242 ± 144	63 ± 5	grey	cylinder
3e	431 ± 35	1754 ± 28	104 ± 9	blue	cylinder
3f	428 ± 40	1503 ± 27	84 ± 9	purple	cylinder
3g	423 ± 44	1475 ± 41	Top: 48 ± 12 Bottom: 113 ± 6	orange/blue	cone
3h	418 ± 34	1339 ± 129	Top: 24 ± 7 Bottom: 123 ± 14	orange/yellow	cone
3i	433 ± 28	690 ± 116	Top: 24 ± 8 Bottom: 105 ± 14	yellow/grey	cone
3j	446 ± 31	470 ± 98	Top: 30 ± 13 Bottom: 92 ± 18	grey	cone

*nanocones were measured at the top

Table S2: Bisegmented VA-SiNW array dimensions.

The dimensions of all synthesized bisegmented VA-SiNW arrays, shown in main text, are reported here. All dimensions are in nm.

Bisegmented SiNW Arrays					
Figure	Array Pitch	SiNW Length		SiNW Diameter	
		Top	Bottom	Top	Bottom
4a	411 ± 42	2632 ± 32	1213 ± 48	69 ± 6	137 ± 6
4b	443 ± 31	407 ± 26	374 ± 43	60 ± 8	143 ± 10
4c	444 ± 38	1337 ± 18	586 ± 28	98 ± 12	133 ± 13

Table S3: Light trapping properties of the synthesized structures.

Summary of the light trapping properties for all synthesized structures. Volumes were calculated based on ideal cylinders or cones and normalized in to the highest structure volume. The reflectance was normalized to the structures volume by multiplying the reflectance at the dip with the normalised volume of each structure.

Figure	Reflectance at Dip [%]	Wavelength at Dip [nm]	Reflectance at 550 nm [%]	Volume [nm³]	Normalised Volume	Normalised Reflectance at Dip
2a	4.3	584	5.2	18580066.96	0.67	2.9
2b	3.8	526	4.5	13030735.71	0.47	1.8
2c	9.4	442	26.8	7930233.585	0.29	2.7
2d	13.7	392	32.5	3871618.676	0.14	1.9
3e	2.8	558	2.9	14899995.9	0.54	1.5
3f	4.7	552	4.7	8329279.47	0.30	1.4
3g	9.7	514	12.1	4930801.7	0.18	1.7
3h	13.5	480	20.6	5303461.6	0.19	2.6
3i	28.9	478	33.0	1991573.4	0.07	2.1
3j	34.1	480	35.2	1041458.9	0.04	1.3
4a	4.4	376	8.6	27722787.2	1.0	4.4
4b	11.3	650	17.6	7157432.4	0.3	2.9
4c	4.5	480	5.6	18226187.0	0.7	3.0

Table S4: Dimensions of the synthesized VA-SiNW arrays used for the reflectance results in Figure 4e.

All dimensions are in nm.

Synthesized VA-SiNW arrays used in Figure 4e					
Sample	Array Pitch (nm)	SiNW Length (nm)		SiNW Diameter (nm)	
		Top	Bottom	Top	Bottom
Exp1 (Fig. 2b)	428 ± 31	2192 ± 49		87 ± 7	
Exp2 (Fig. 2a)	418 ± 42	1699 ± 41		118 ± 5	
Bi-segmented	444 ± 38	1337 ± 18	586 ± 28	98 ± 12	133 ± 13

Table S5: Dimensions of the simulated VA-SiNW arrays used for the results shown in Figure 4f (averaged over 8 different wire diameters)

All dimensions are in nm.

Simulated VA-SiNW arrays used for the results shown in Figure 4f-h					
Sample	Array Pitch	SiNW Length		SiNW Diameter	
		Top	Bottom	Top	Bottom
Sim1	420	2200	n.a.	87 ± 7*	n.a.
Sim2	420	1700	n.a.	118 ± 5*	n.a.
Bi-segmented	450	1400	600	100*	130*

* Includes a 3 nm SiO_2 layer (i.e. a 100 nm diameter corresponds to a 94 nm diameter with 3 nm SiO_2 on each side of the wire)

Table S6: Dimensions of the simulated VA-SiNW arrays used for the results shown in Figure 4g-h (all three wires have the same volume)

All dimensions are in nm.

Simulated VA-SiNW arrays used for the results shown in Figure 4f-h					
Sample	Array Pitch	SiNW Length		SiNW Diameter	
		Top	Bottom	Top	Bottom
Sim1	450	2414	n.a.	100*	n.a.
Sim2	450	1428	n.a.	130*	n.a.
Bi-segmented	450	1400	600	100*	130*

* Includes a 3 nm SiO_2 layer (i.e. a 100 nm diameter corresponds to a 94 nm diameter with 3 nm SiO_2 on each side of the wire)

Materials and chemicals

All chemicals and solutions were used without further processing, unless noted otherwise. Acrylic acid (99.0 %), ammonium hydroxide (28-30 %, NH_3 basis), ammonium persulfate (APS, 98.0 %), ethanol (99.9 %), iodine (99.8 %), N-Isopropylacrylamide (NiPAm, 97%), potassium iodide (99.8 %), styrene (99.0 %), tetraethyl orthosilicate (TEOS, 98%) and 3 trimethoxy propyl methacrylate (MPS, 98 %) were purchased from Sigma Aldrich, USA. NiPAm was purified by recrystallization from hexane. Styrene was purified by adding a 10 wt-% NaOH solution in a volume ratio 1:1. After vigorous shaking, the aqueous phase was discarded, and the styrene phase purified by passing through an aluminum oxide powder column. Acetone (technical grade), ethanol (euro denaturated 96 %) and *n*-hexane (Technical) were purchased from VWR, Europe. Hydrofluoric acid (40 %, EMSURE), hydrogen peroxide (30 % ACS grade) and potassium hydroxide (pellets GR for analysis) were purchased from Merck, Germany. N-doped silicon wafers (100) (resistivity

1 – 30 Ωcm) were purchased from Si Materials, Germany. The water used was double deionized using a MilliQ system with a resistivity of 18 MΩ.

Synthesis protocols

Two different types of colloidal particles were used for the colloidal lithography. For nanowires with small diameters (d < 160 nm), SiO_2-PNIPAM core-shell particles were used. For nanowires with large diameters (d > 160 nm, Figure S1), polystyrene (PS) particles were used.

Colloidal lithography using SiO_2 - PNIPAM core-shell particles

Particle Synthesis: SiO_2 - PNIPAM core-shell particles were synthesized, self-assembled at the air/water interface and used as mask as described elsewhere.[1] In short, silica nanoparticles with a diameter of 160 nm (±10 nm) were prepared according to the Stöber process. The silica nanoparticles were functionalized with 102.7 µL 3(trimethoxysilyl)propyl methacrylate (MPS) under stirring at room temperature for at least 1 day and subsequent boiling for 1 h to ensure successful functionalization. Afterwards, the particles were purified by centrifugation and redispersed three times in ethanol and three times in Milli-Q water. A PNIPAM microgel shell was polymerized on the synthesized silica nanoparticles *via* surfactant-free precipitation polymerization. The core-shell particles were purified by centrifugation and redispersion with Milli-Q water.

Self - Assembly: The SiO_2- PNIPAM core-shell particles were self-assembled at the air/water interface using a Langmuir-Blodgett trough (KSVNIMA) (area = 243 cm², width = 7.5 cm) with Delrin barriers and the surface pressure was measured by a Wilhelmy plate. The N-type silicon wafers were cut into ~ 8 x 1.5 cm² and cleaned by ultrasonication in acetone, ethanol and Milli-Q water for 4 min each, followed by oxygen plasma (Diener) cleaning. Four substrates were mounted

vertically onto the dipper and the trough was filled with Milli-Q water. The core-shell particle suspension was diluted to 0.5 wt %, mixed with 30 wt % ethanol as the spreading agent, and spread at the air/water interface of the trough using a regular 100 µL pipette. After 10 min of equilibration, the barriers were compressed to a constant surface pressure of 30 mN/m while the dipper was lifted by 0.8 mm/min. After deposition, the SiO_2- PNIPAM core-shell particles were exposed to oxygen plasma for 10 min to remove the organic PNIPAM shell, leaving a non-close packed array of silica particles at the surface.

Colloidal lithography using polystyrene (PS) particles

Particle Synthesis: PS colloids with a diameter of 590 nm were synthesized using surfactant – free emulsion polymerization. In short, in a 500 mL triple-neck round-bottom flask with reflux-condenser, 250 mL of MilliQ water were heated to 80 °C. Nitrogen gas was bubbled for 30 min for degassing. Then, 20 g styrene was added to the water phase under constant stirring, followed by the addition of 0.4 g of the comonomer acrylic acid dissolved in 5 mL MilliQ water. After 5 min, 0.1 g ammonium persulfate dissolved in 5 mL MilliQ water was added to initiate the polymerization. The reaction was carried out for 24 h at 80 °C. After cooling to room temperature, the dispersion was filtered and purified by centrifugation and redispersion and dialysis against MilliQ water.

Self - Assembly: The PS colloidal particles were self-assembled at the air/water interface using ethanol as a spreading agent.[2] Prior to the interfacial self-assembly process, the PS colloids were cleaned and purified by three centrifugation-redispersion steps using 1:1 ethanol/water mixtures to avoid amphiphilic impurities present in colloidal dispersions.[3] For the spreading onto air/water interface 750 µL of PS colloid dispersion was mixed with 250 µL ethanol. The dispersion was filled into a syringe and added to the water surface using a syringe pump (Landgraf HLL LA120)

at a speed of 30 µL/min. N-type c-Si substrates were cut into 4 x 4 cm² pieces and cleaned via sonication in acetone, ethanol and MilliQ water for 4 min each, followed by cleaning using oxygen plasma. The silicon substrates were immersed in the water phase and lifted through the air/water interface to deposit the monolayer of PS colloidal particles onto the substrate. Then the substrate was positioned under a steep angle and dried in air. The procedure yielded large-area colloidal crystals with grains in the mm² range. After monolayer deposition, the colloidal particles were exposed to oxygen plasma (FEMTO; Diener Electronic, 50 W, oxygen flow 4 mL/min) for 14 min to reduce their size from d = 590 nm to d = 410 nm, forming a non-close packed monolayer at the substrate.

Synthesis of VA-SiNW arrays *via* metal-assisted chemical etching (MACE)

Metal deposition: A thin adhesion layer of Al doped ZnO was sputtered directly on the non-close packed colloids, using a Clustex 100M sputtering system from Leybold Optics: base pressure before deposition around 1.10^{-6} mbar, Ar pressure during deposition 3.10^{-3} mbar, 1 s deposition, power 75 W for colloids with d < 160 nm (silica particles) and 100 W for colloids with d > 160 nm (PS particles). The samples were then immediately sputtered with a gold film using a Cressington Sputter Coater 108 auto (deposition at 40 mA during 300 s). Finally the PS or silica particles were removed using adhesive tape (Scotch Magic Tape) and cleaned with oxygen plasma (Emtech K1050X) at 50 W for 5 min with an oxygen flow of 10 mL/min.[4,5]

Metal-assisted chemical etching: MACE was used to prepare Si nanowires by immersing the Si/Au hole array substrates in an aqueous HF/H_2O_2 mixture. *Caution: Appropriate safety precautions have to be observed when working with hydrofluoric acid (HF): HF is a contact poison!* The MACE solution was prepared fresh before etching. Typically, the substrates were placed on a home-made 3D printed polymer sample holder and immersed into the etching solution for the

desired duration. The MACE solution was composed of 10 mL of hydrofluoric acid, 10 mL of MilliQ water, and 0.75 ml of hydrogen peroxide. Typical etching durations were 2 – 7 minutes depending on VA-SiNW length. The substrates were then rinsed three times with MilliQ water, once with ethanol and finally dried in air. After drying, the samples were immersed into a solution composed of 20 mL of MilliQ water and 4 mL of hydrofluoric acid to remove residual porous SiO_2 which can be formed on the sidewalls of the VA-SiNW during MACE. The substrates were then rinsed three times with MilliQ water, once with ethanol and finally dried in air. The substrates were stored or immediately used. For the diffuse reflectance measurements, the gold film was etched in a KI/I_2 aqueous solution (10 wt. % KI, 5 wt. % I_2).

Characterization Methods

Diffuse reflectance measurements

Diffuse reflectance measurements were performed using a Perkin Elmer Lambda 1050 equipped with a 150 mm integrating sphere (PbS + InGaAs detector) with an adjustable circular aperture and a focusing lens. Both spectral and diffuse reflected light was collected from 300 – 1500 nm. Before measurements, the gold film at the bottom of the VA-SiNW (from MACE) was etched in a KI/I_2 solution (10 wt. % KI, 5 wt. % I_2). The substrate was placed onto the sample holder with a circular pinhole. For the monosegmented (Fig. 2) and bisegmented (Fig. 4) nanowires a pinhole with a diameter of 5 mm was used. For the macroscale gradient (Fig. 3) a pinhole with a diameter of 3 mm was used. Before measuring samples, a 100% transmission reference spectrum was taken by placing a white reference (Spectralon) behind the pinhole. The size of the light beam was adjusted to the pinhole diameter. During measurement of the samples, the white reference was placed behind the substrate to reflect the transmitted light (only IR radiation). 3 measurements were taken at different spots on the sample and the mean value was taken. Typical deviations in

the visible were about ± 0.3 % and about ± 2-3 % in the IR region. For the sample with size and dimension gradient at the macroscale, the sample was aligned to the pinhole and moved by 1 mm for each measurement. Only one spectrum was recorded to preserve the alignment. Figure S3 shows a photograph of the gradient sample and the area used for diffuse reflectance measurements is highlighted.

FDTD simulations

The electromagnetic simulations were performed using a commercially available finite-difference-time-domain (FDTD) simulation software package (Lumerical Solutions Inc., Vancouver, Canada). Unless indicated otherwise, periodic arrays of nanowires were modelled: One unit cell was simulated using periodic boundaries along the x- and y-axis, while infinite boundary conditions rendered as perfectly matched layers (PML) were used along the z axis. The nanowires were located on bulk silicon. A plane wave source was injected above the array, propagating in the z-direction, parallel to the wire longitudinal axis with the electric field perpendicular to the wire longitudinal axis (along the x-axis). The simulations were done in three-dimensions. The distance between the structures investigated and the simulation boundaries were at least half the simulation wavelength. The refractive index of the medium was set to 1 (air). A 3 nm conformal SiO_2 shell was added around the nanowires to take into account the effect of the native oxide. This slightly blue-shifts the reflectance dips, since it slightly reduces the Si wire diameter. The reflectance (R) spectra were modelled using a 2D power monitor located above the array. The dielectric constants of silicon and SiO_2 were used directly from the Lumerical materials library: we used Palik's data for silicon and SiO_2.[6]

Additional information concerning the simulations:

Gradient sample (Figure 3). Based on our SEM cross-sectional images, we have introduced a small tapering to simulate the wires located at the beginning of the gradient (almost unetched by KOH, location Figure 3e): These wires were modelled with a top diameter that is 10% smaller than the bottom diameter.

Bisegmented nanowires (Figure 4).

Figure 4f. The simulated spectra shown on Figure 4f were obtained by using the same array pitch and wire length as the synthesized arrays used for Figure 4e. However they take into account the small variations in wire diameter across the samples and were obtained by averaging the simulated spectra of 8 arrays with different diameters, based on the size distribution obtained from SEM analysis. A slight tapering of the wire was also taken into account. The single diameter wires had a 10% tapering (i.e. the top diameter was 10% smaller than the bottom diameter). The top segment of the bisegmented wire arrays had a 10% tapering, while the bottom segment had a 5% tapering. Both tapering are justified. The top segment was etched in KOH, which can lead to a small tapering of the wires (i.e ~ 10%). The small 5% tapering after MACE is justified by the fact that Si slowly dissolves in HF, while the gold template can also slightly change in dimensions over the etching experiment. Taken together this can lead to a slightly different in diameter at the top and bottom of the wires after MACE.

Figure 4g. Figure 4g shows the effect of diameter and bi-segmentation on the array absorptance. The simulated reflectance and transmittance spectra were obtained from ideal structures (no size averaging, no tapering), and the length of the simulated wires was chosen to obtain the same volume for all three simulated structures, thus allowing direct comparison of the optical data. The

transmittance (T) spectra were modelled using a 2D power monitor located within the silicon substrate at 80 nm below the surface. The absorptance (A) spectra were calculated from T and R as: $A = 1 - R - T$. Thus, there is a constant baseline to the absorptance for all spectra shown on Figure 4g that comes from this 80 nm thick silicon layer. The experimental and simulated wire lengths can be compared with tables S4 and S6. The reflectance, transmittance and absorptance spectra are shown in Figure S9.

The increase in absorption discussed in the main text between the mono- and the bisgemented nanowires was calculated by integrating the absorptance spectra over the 375 – 825 nm wavelength range.

Figure 4h. The relative absorption maps shown in Figure 4h were obtained using the advanced power analysis group of Lumerical, which provides the local absorbed power density (P_{abs}) in three dimensions. Only the 2D maps are shown, corresponding to the cross-section going through the center of the wire in the x-z plane at y = 0. These maps were normalized to obtain the relative absorption.

Figure S10. The relative charge carrier photogeneration rate G maps shown in Figure S10 were obtained by simulating a single nanowire on Si (i.e. not the periodic array), using the same orientation and geometry as the ones used for the arrays. G was obtained by normalizing the P_{abs} maps, assuming that every absorbed photon generates one electron-hole pair.

Optical Microscopy

Optical microscopy images of the arrays were acquired using a Zeiss Axio Imager M2m. Images were taken with a 10x objective under bright field conditions.

Scanning Electron Microscopy

Secondary electron (SE) SEM images of the arrays were acquired using a Zeiss Ultra Plus at a working distance of ~ 2.5 - 4 mm, equipped with an InLens SE detector. The accelerating voltage was adjusted between 1 and 5 kV, depending on the sample, to limit charging.

Figures

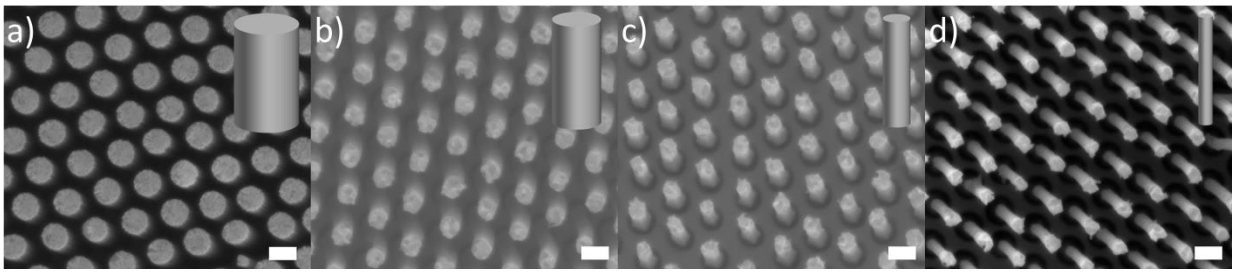

Figure S1. KOH Etching of VA-SiNW Arrays with pitch = 590 nm and nominal diameter = 411 nm.

Top view SEM images of homogeneously etched VA-SiNW with a pitch of 590 nm using an aqueous 20 wt. % KOH solution. 4 different samples were taken and etched for 0 s, 10 s, 20 s, 30 s. After SEM imaging, each sample was further etched for 40 s. No HF pre-treatment was done before KOH etching. (a) 0 s KOH; d = 411 nm. (b) 30 s KOH; d = 289 nm (c) 60 s KOH; d = 235 nm (d) 90 s KOH; d = 209 nm. Scale bars: 400 nm. *Note: The VA-SiNW arrays with diameter < 150 nm shown in Figure 2 were etched in a single step using 0.2 wt. % KOH.*

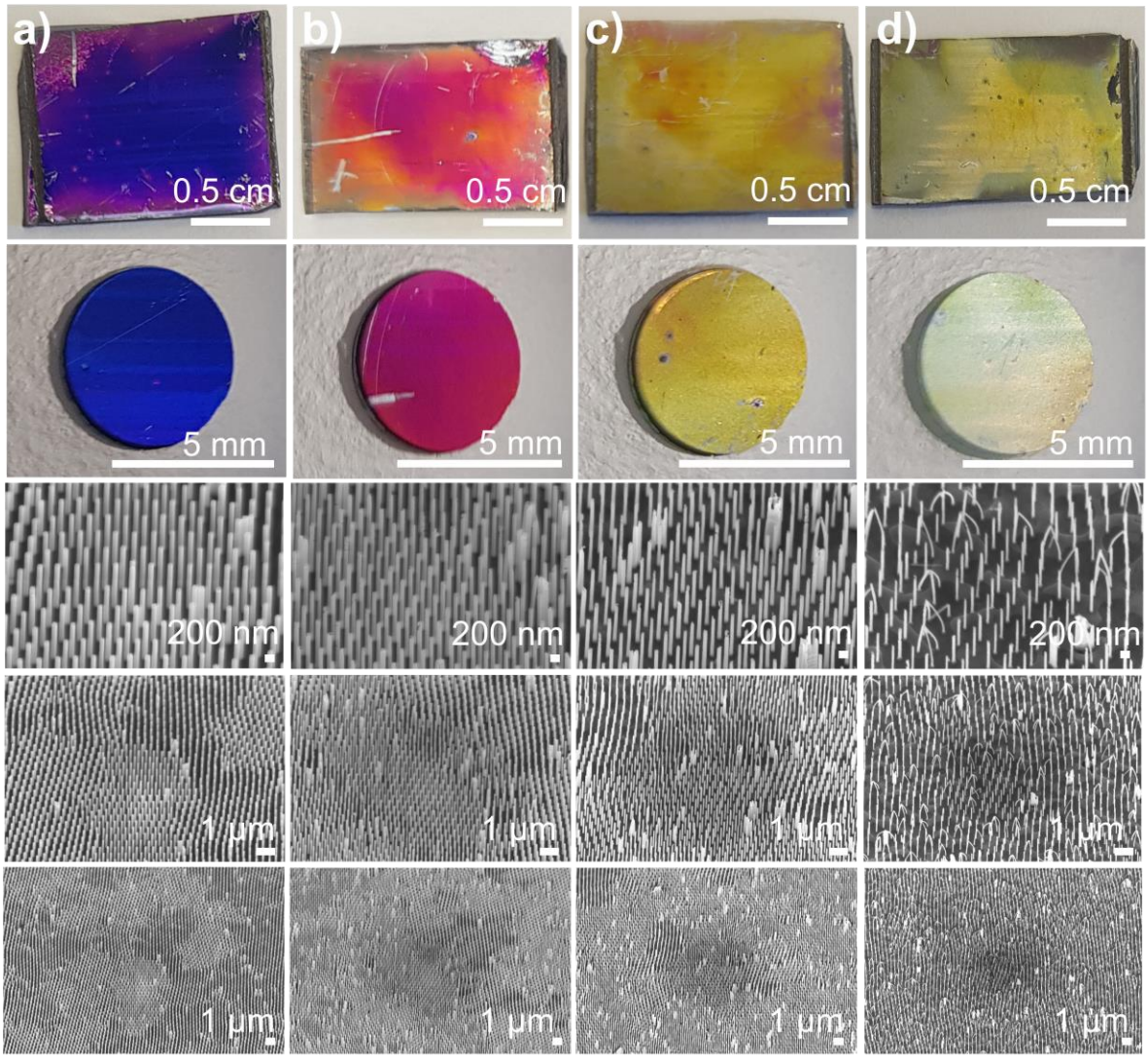

Figure S2. Large-scale homogeneity of diameter-controlled SiNW arrays by KOH etching from Figure 2.

(a-d) Substrates from Figure 2a-d. Top Row: Photograph. Second Row: Area used for UV-Vis measurements. Last Rows: Secondary electron SEM images in different magnifications. (a) Reference substrate after MACE with d = 118 nm. (b) SiNW array with d = 87 nm after 20 s KOH etching. (c) SiNW array with d = 77 nm after 40 s KOH etching. (d) SiNW array with d = 63 nm after 60 s KOH etching.

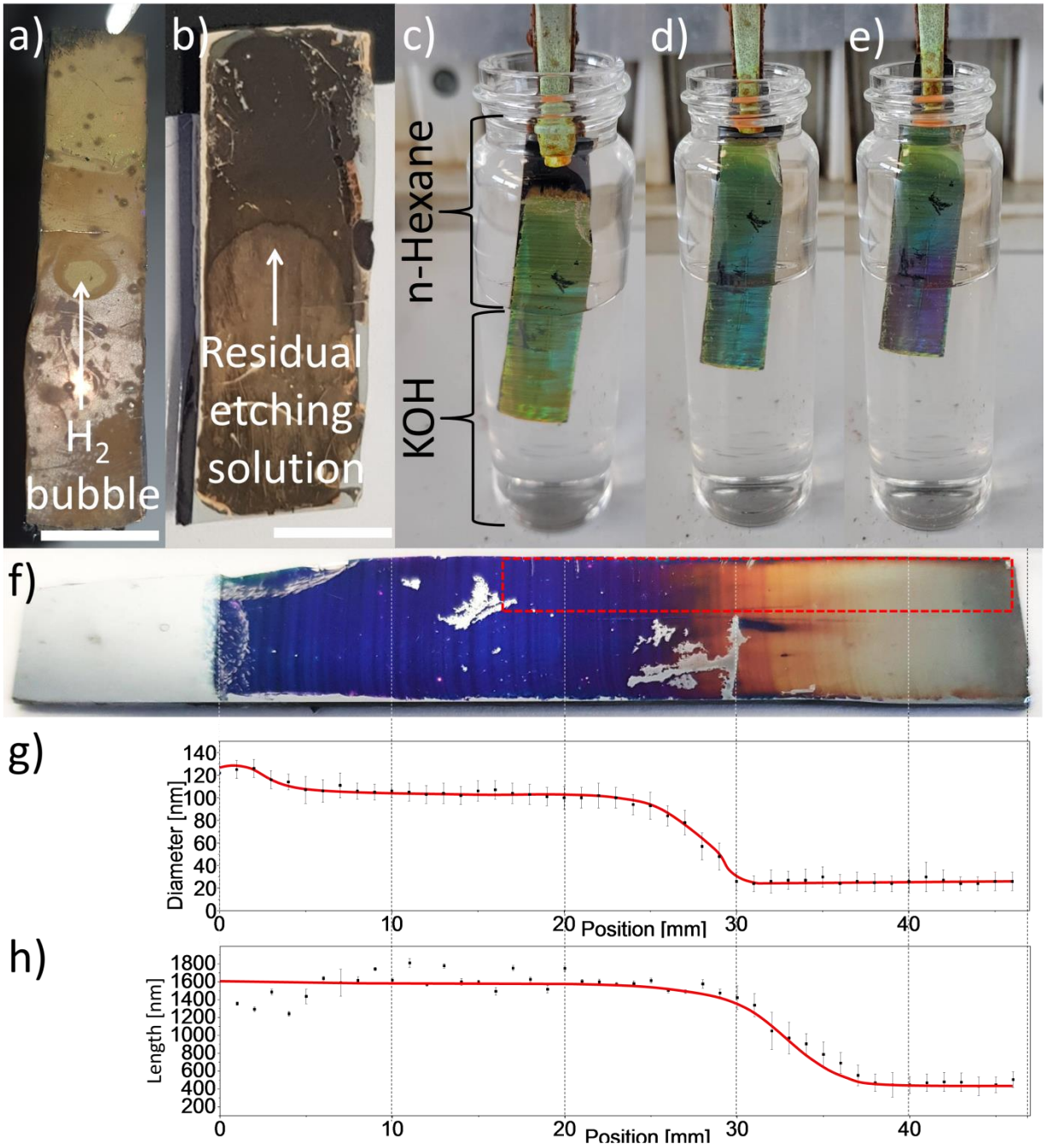

Figure S3. Dip-etching.

(a) Photograph of a substrate with local inhomogeneity due to a large H_2 bubble when using a high concentration of KOH (1 wt. %). Removal rate (200 mm/h). Scale bar: 1 cm. (b) Photograph of a substrate with local inhomogeneity due to residual etching solution after removal from solution

(i.e. dip-etching was performed in a one-phase system, without an additional *n*-hexane layer on top). Scale bar: 1 cm. (c-e) Photographs during the dip etching at different times. A low concentration (0.2 wt. %) and slow removal rate was utilized (200 mm/h) to prevent the formation of large H_2 bubbles. A *n*-hexane phase on top of the KOH solution helped to limit residual KOH solution trapped in the wires. (f) Photograph of the gradient sample. The area of the cropped image shown in Figure 3 is highlighted (dashed red rectangle) and was further analyzed by diffuse reflectance measurements. (g, h) Evolution of the nanowire morphology across the sample. The nanowire diameter (g) and length (h) were measured every millimeter. The red lines are guides to the eye.

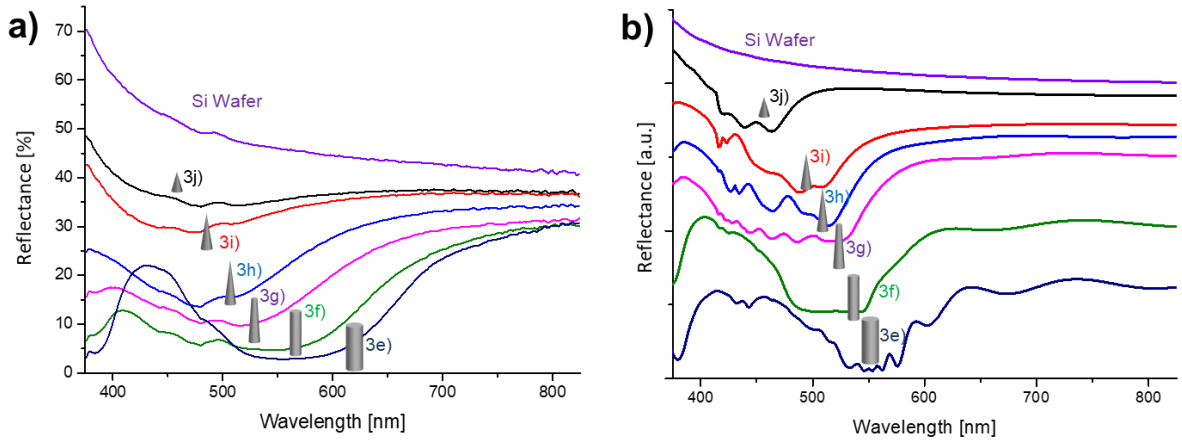

Figure S4. Diffuse reflectance spectra of the macroscale gradient sample.

(a) Experiment. Raw data (no offset). (b) Simulation. The spectra were offset for clarity.

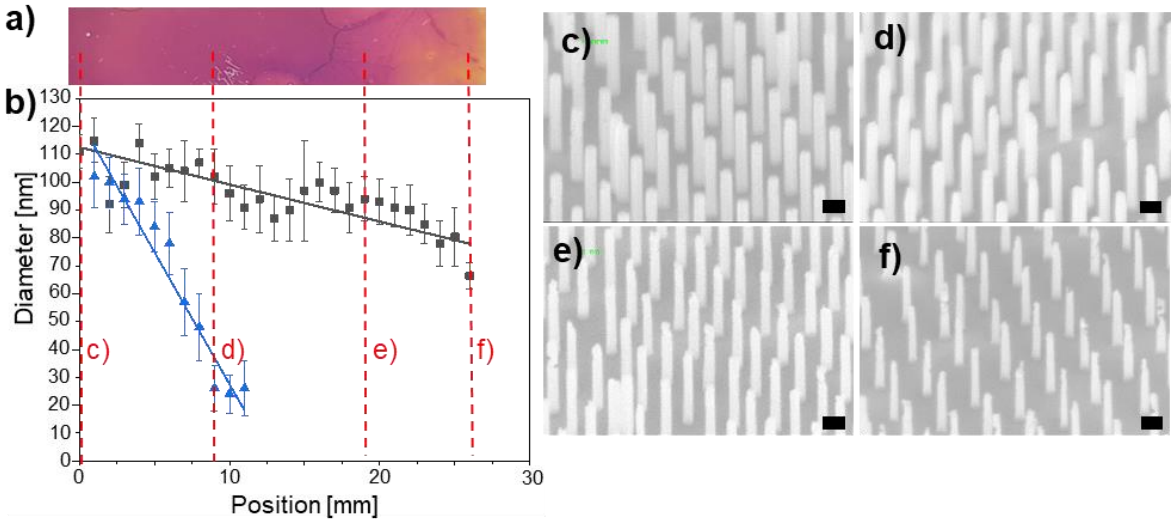

Figure S5. Diffuse reflectance spectra of the macroscale gradient sample.

(a) Photograph of a gradient substrate fabricated with a faster removal rate (4000 mm/h). (b) Evolution of nanowire diameter across the sample (black symbols and line). The blue symbols and line represent the gradual changes from the substrate from Figure 3, S3, which was removed with a much slower rate (200 mm/h). The rate of decrease in diameter was around 1.3 nm/mm for the black line and 9.5 nm/mm for the blue line. (c-f) Secondary electron SEM images showing different locations on the substrate. Tilt angle 45 °. Scale bars: 200 nm.

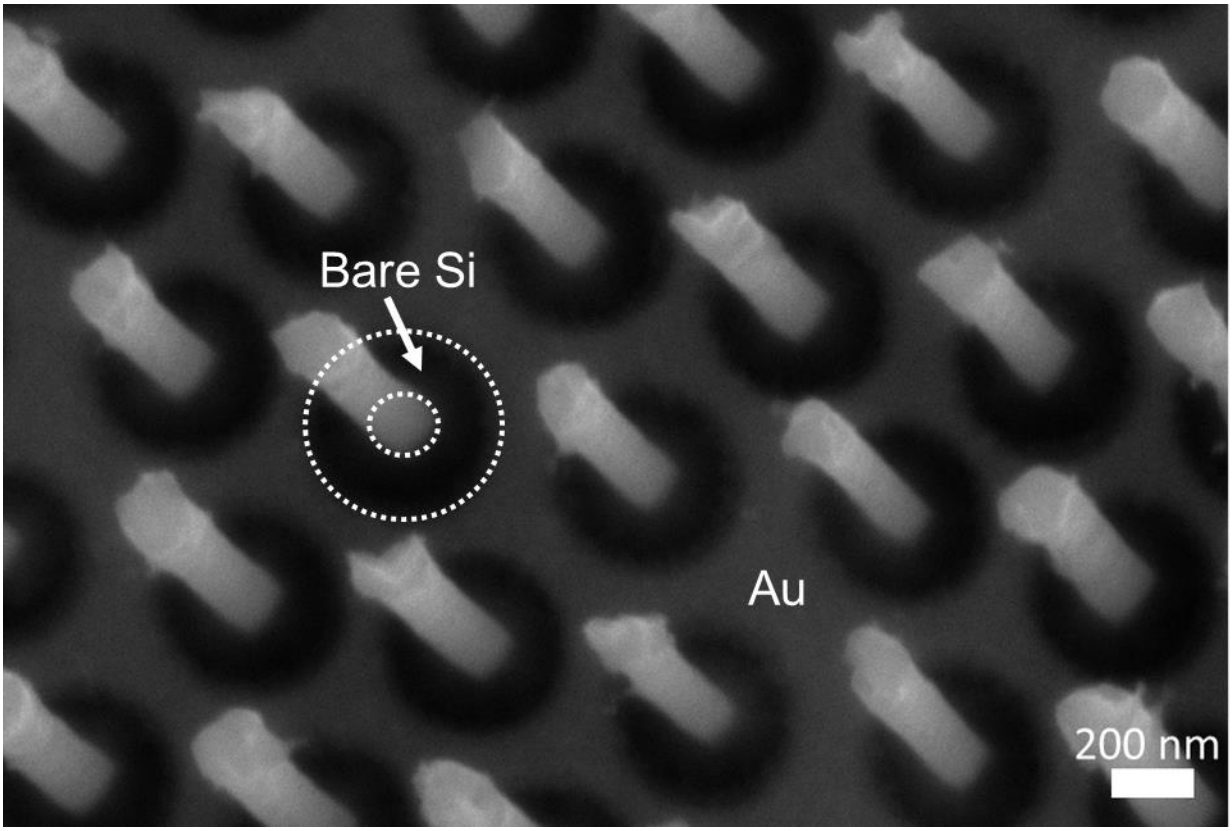

Figure S6. Stability of Au nanohole film present at the bottom of the VA-SiNW during KOH etching.

Secondary Electron SEM image. Tilt angle = 30 °. The black circular areas at the bottom of the Si wires highlighted with white dashed circles correspond to bare silicon, exposed after KOH etching. The lighter areas surrounding these darker areas correspond to the original gold nanohole film, which is still there and does not delaminate during KOH etching.

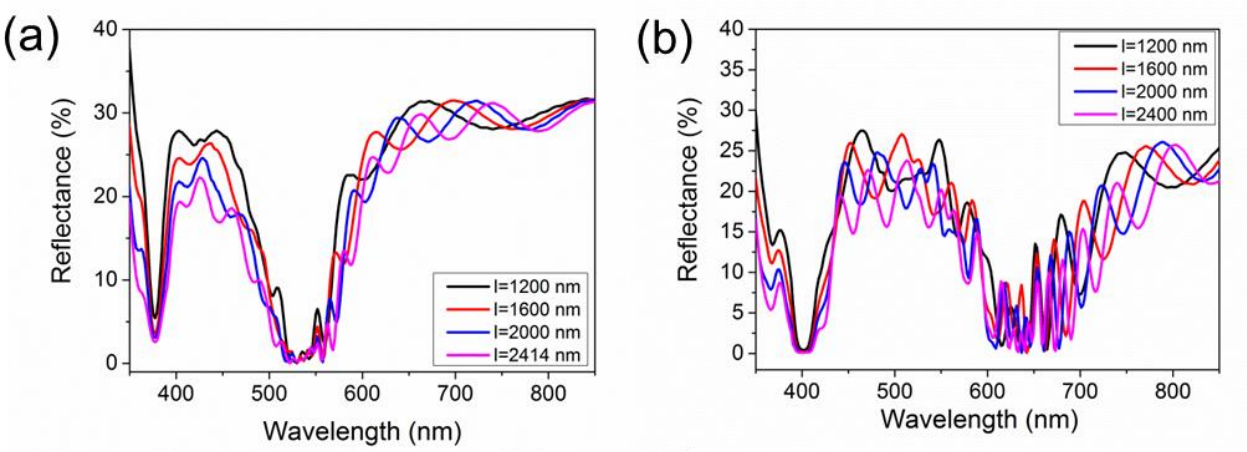

Figure S7. Simulations results: Effect of length on the reflectance spectra of VA-SiNW arrays with diameters of 100 nm (a) and 130 nm (b). Array periodicity: 450 nm. No tapering.

The closely spaced oscillations due to Fabry-Pérot resonances are clearly length-dependent. The location of the reflectance minima however is not affected by the nanowire length and only depends on the wire diameter. Overall, the spectrum envelops are not affected by the wire length.

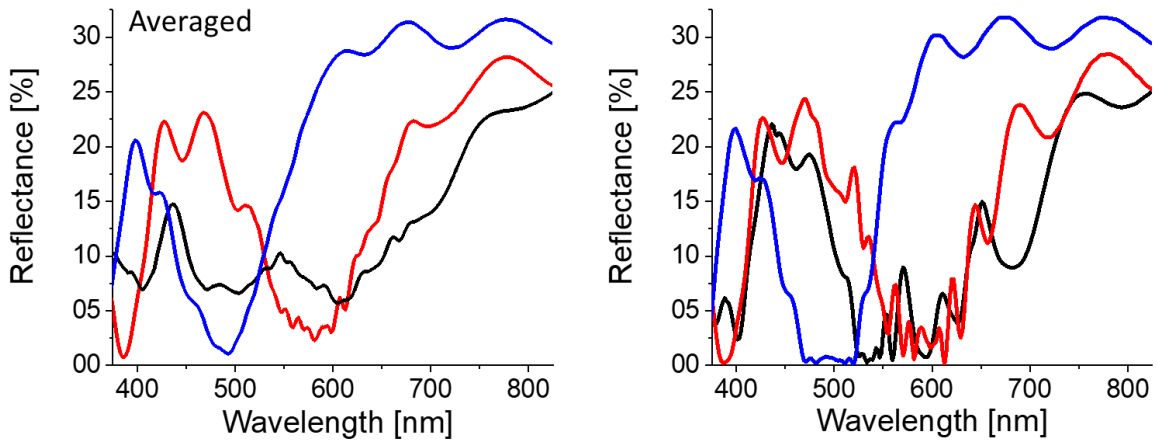

Figure S8. Simulations results: Effect of averaging over several different diameters to take into account the array size distribution.

Left: Simulated reflectance spectra shown in Figure 4f, obtained by averaging over different diameters to take into account the wire size distribution. Black curve: bisegmented VA-SiNWs d_{top} = 100 nm and d_{bottom} = 130 nm. Red curve: single diameter VA-SiNWs with d_{exp1} = 87 nm. Blue curve: single diameter VA-SiNW with d_{exp2} = 118 nm.

Right: Simulated reflectance spectra of the same structures, same color code. No average (single structure spectra, i.e. just one diameter).

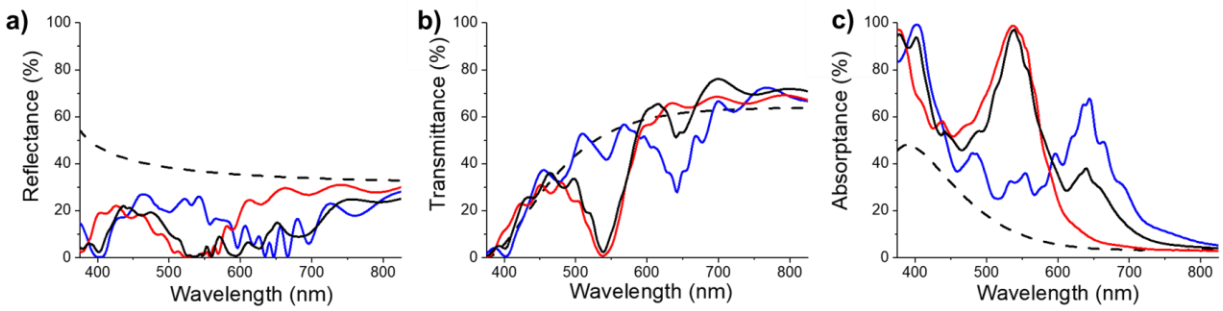

Figure S9. Simulated reflectance, transmittance and absorptance spectra of bisegmented nanowires simulated on Figure 4g (not averaged over different diameters, no tapering).

All structures have the same volume. The transmittance spectra were obtained 80 nm below the surface of the silicon substrate. Thus the transmittance and absorptance spectra include the contribution of the wires + 80 nm of bulk silicon. The thickness of the bulk silicon sample was thus 188 nm, corresponding to 108 nm on top of 80 nm. Dashed black curve: 108 nm thick bulk silicon on top of 80 nm Si (i.e. total of 188 nm thick bulk Si). Black curve: bisegmented VA-SiNW $d_{\text{sim, top}}$ = 100 nm and $l_{\text{sim, top}}$ = 1400 nm, $d_{\text{sim, bottom}}$ = 130 nm and $l_{\text{sim, bottom}}$ = 600 nm; Red curve: single diameter VA-SiNWs with d_{sim1} = 100 nm and l_{sim1} = 2414 nm. Blue curve: single diameter VA-SiNWs with d_{sim2} = 130 nm and l_{sim2} = 1428 nm.

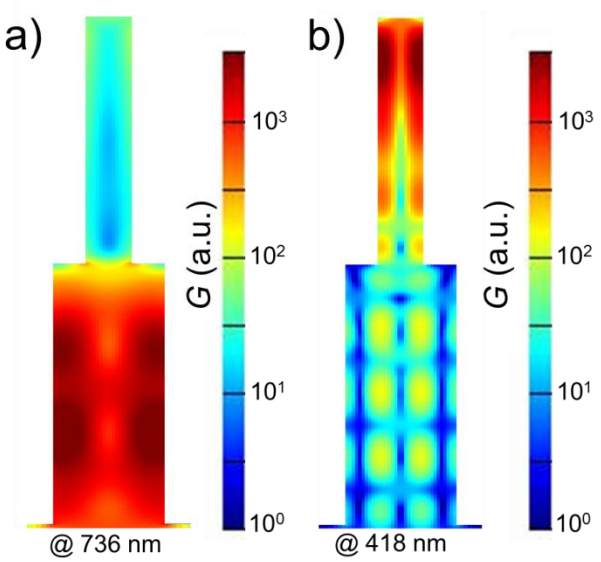

Figure S10. Simulated maps of the relative charge carrier photogeneration rate *G* within a single wire with dimensions corresponding to the array shown in Figure 4c (i.e. d_{top} = 60 nm and d_{bottom} = 140 nm). At 736 nm (a), most charge carriers are generated at the bottom of the segment due to its larger diameter, while at 418 nm (b), most charge carriers are generated in the top segment. N.B.: the values of *G* are relative and valid for one map only; they cannot be compared between the two maps.

References

1. Tang, J. S. J. *et al.* Surface Patterning with SiO_2@PNiPAm Core-Shell Particles. *ACS Omega*, **2018**, 3, 12089–12098; DOI:10.1021/acsomega.8b01985
2. Vogel, N., Goerres, S., Landfester, K. & Weiss, C. K. A Convenient Method to Produce Close- and Non-close-Packed Monolayers using Direct Assembly at the Air-Water Interface and Subsequent Plasma-Induced Size Reduction. *Macromol. Chem. Phys.*, **2011**, 212, 1719–1734; DOI:10.1002/macp.201100187
3. Rey, M., Yu, T., Guenther, R., Bley, K. & Vogel, N. A Dirty Story: Improving Colloidal Monolayer Formation by Understanding the Effect of Impurities at the Air/Water Interface. *Langmuir*, **2019**, 35, 95–103; DOI:10.1021/acs.langmuir.8b02605
4. Wendisch, F. J., Oberreiter, R., Salihovic, M., Elsaesser, M. S. & Bourret, G. R. Confined Etching within 2D and 3D Colloidal Crystals for Tunable Nanostructured Templates: Local Environment Matters. *ACS Appl. Mater. Interfaces*, **2017**, 9, 3931–3939; DOI:10.1021/acsami.6b14226
5. Wendisch, F. J. *et al.* Three-Dimensional Electrochemical Axial Lithography on Si Micro- and Nanowire Arrays. *Nano Lett.*, **2018**, 18, 7343–7349; DOI:10.1021/acs.nanolett.8b03608
6. Palik, E. D. *Handbook of optical constants of solids* (Academic Press, San Diego, 1998).